Indian Ocean impact on ENSO evolution 2014-2016 in a set of seasonal forecasting experiments

Supplementary Material

Michael Mayer[1,2,*] and Magdalena Alonso Balmaseda[1]

[1]Research Department, European Centre for Medium-Range Weather Forecasts, Reading, UK

[2]Department of Meteorology and Geophysics, University of Vienna, Vienna, Austria

[*]corresponding author address:

ECMWF

Shinfield Rd

Reading RG2 9AX

michael.mayer@ecmwf.int

S1. Contrasting atmosphere-ocean evolution in 2014-2016 with 1997-1999

Despite the failure of SEAS5 to correctly predict the evolution during 2014-2016 in an ensemble mean sense, the system's forecast was clearly distinct from that for 1997-1999. In fact, the system is quite successful in predicting the differences with the 1997-1999 evolution. This is demonstrated in Fig. S1, which compares the difference of the 2014-2016 and the 1997-1999 in (upper row) the forecasts and (lower row) reanalysis.

In 1997, the observed year-1(Y1) Pacific SST anomalies were comparatively warmer than in 2014, while they were comparatively colder during year-2 (Y2). Panels (Fig. S1a and e) show that this feature is correctly captured by the forecast experiments, as well as the associated mechanisms and timing. For instance, the relative warming in observations in Y1 is associated with typical features of the onset of El Niño event in the first few months (boreal spring-summer): westerly wind anomalies in the central Pacific (Fig. S1c and g) and the signature of associated upper level divergence around the maritime continent (Fig. S1d and h), and eastward propagating Kelvin waves in ocean heat content (Fig. S1b and f). These features that arise mainly from the onset of the 1997/98 El Niño event are well captured by the forecasts. The forecast also reproduces the evolution into the mature phase by the end of Y1: SST amplification on the Eastern Pacific and subsequent westward propagation (in form of reflected Rossby waves), persistent westerlies around the dateline linked to the eastward displacement of the convection, and establishment of a strong zonal dipole in the Equatorial Pacific Ocean Heat content anomalies. It is worth noting that by boreal autumn of Y1, the Eastern Indian Ocean develops a positive IOD event in 1997/98, with suppressed convection, and strong easterlies that appear to trigger a westward propagating upwelling Rossby wave emanating from the maritime continent. The forecasts also capture the demise of the relative warming during Y2, and the onset of relatively cold conditions in the Pacific.

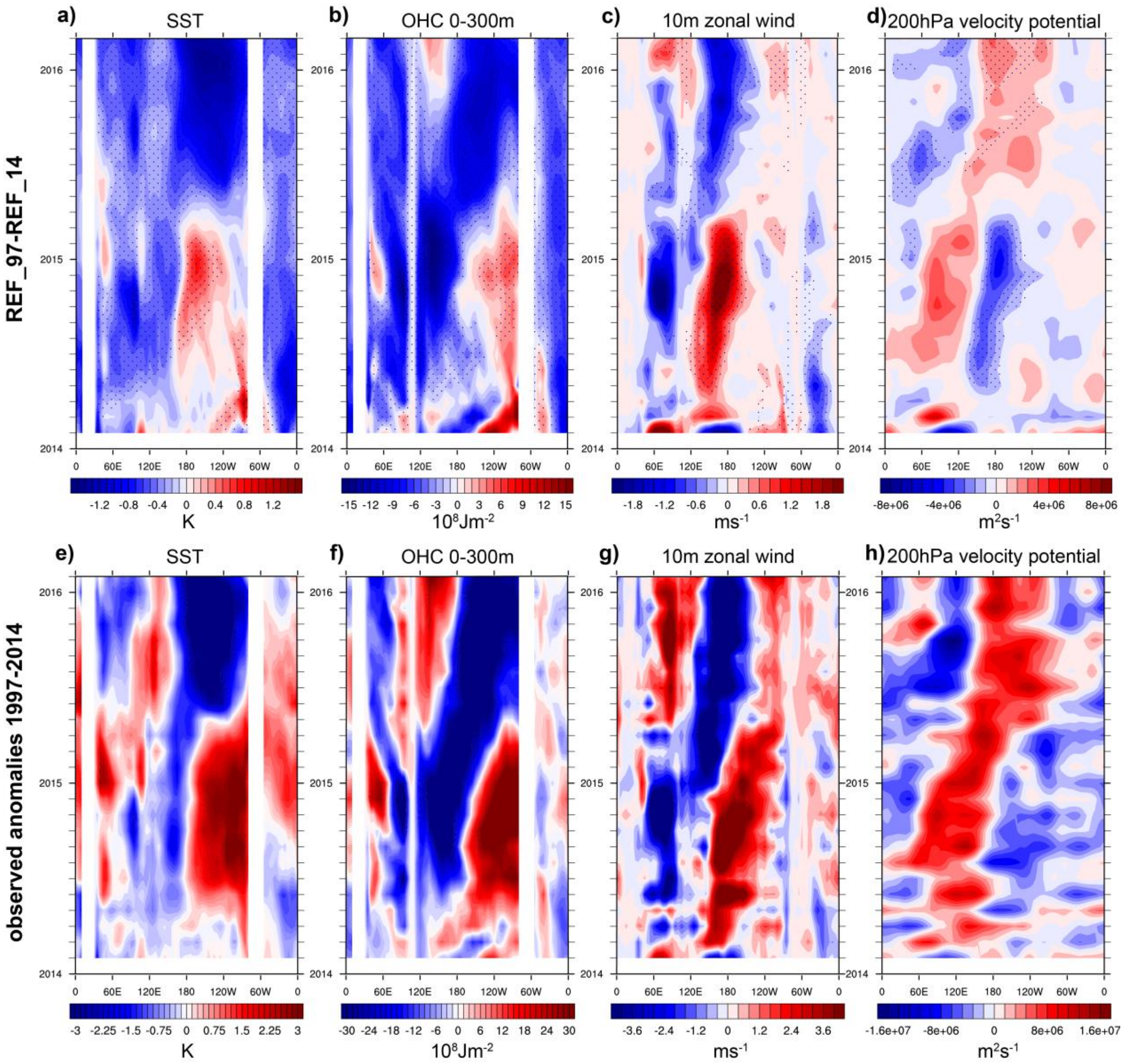

Fig. S1. Longitude-time Hovmoeller diagrams of anomaly differences between 1997-1999 and 2014-2016 in (upper row) forecasts (REF_97-REF14) and (lower row) reanalysis (ORAS5 and ERA-Interim). Shown are equatorial (5S-5N) (a) SST, (b) 0-300m OHC, (c) 10m zonal winds, (d) 200hPa velocity potential, (e) SST, (f) 0-300m OHC, (g) 10m zonal winds, and (h) 200hPa velocity potential.

S2. Spatial structure of Ocean Heat Content Evolution in IndO_97

Fig. S2 illustrates the spatial evolution of differences in upper 300m ocean heat content (OHC) between IndO_97 and REF_14 at different lead times. As expected from the experiment setup, the main differences during lead month one are confined to the Indian Ocean (a), which is much cooler in IndO_97 than in REF_14. During Oct 2014 – Feb 2015 (b), differences are already present in the tropical Pacific, which is warmer in the east and colder in the west in IndO_97 compared to REF_14. This is indicative of a flatter thermocline and warmer ENSO conditions in IndO_97 (a discussion of Niño 3.4 anomalies is provided in main text 3.1.3). By May 2015 – Sep 2015 (c), negative differences dominate along the equatorial Pacific, with only weakly positive differences in other areas of the Pacific. Differences during Oct 2015 – Feb 2016 (d) are similar, with the negative values confined more to the eastern Pacific. The entire Indo-Pacific tropical ocean average OHC differences in Fig. S2a-d is relatively stable around $-4x10^{8}Jm^{-2}$ (see numbers at the top of every subplot), which suggests that the tropical average OHC difference remains roughly stable, but that a significant fraction of the negative OHC anomaly in the IndO_97 ocean initial conditions is transferred to the Pacific. See main text section 3.2 for a quantification of the tropical Pacific heat budget.

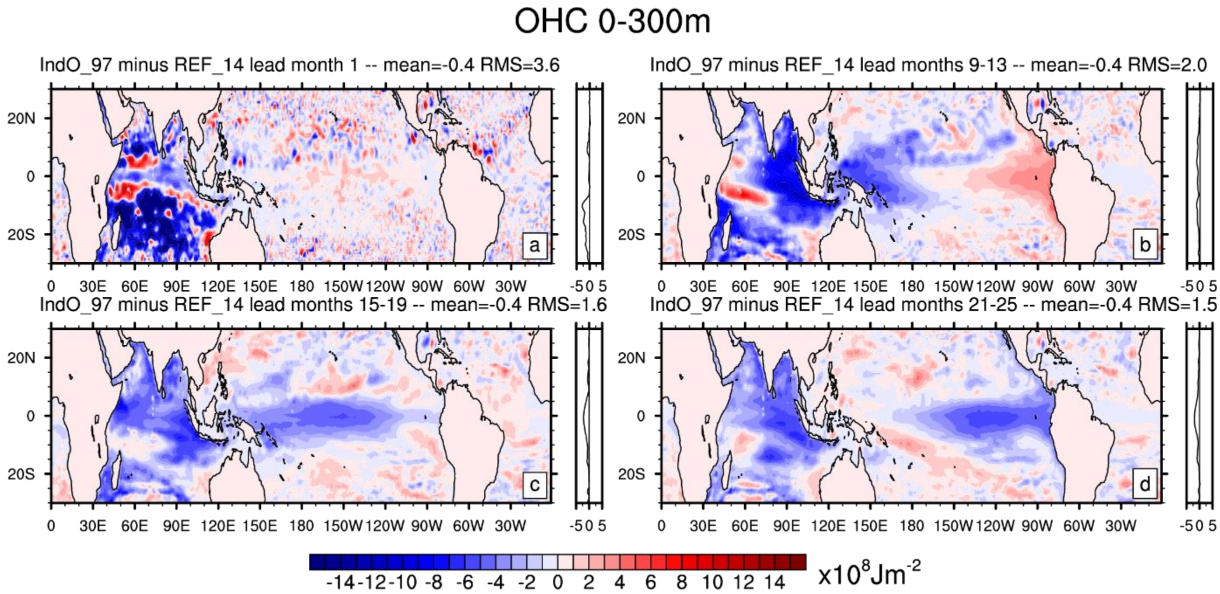

Fig. S2 Temporal evolution of 0-300m OHC difference between IndO_97 and REF_14 at different lead times: a) lead month 1 (=Feb 2014), b) five-month average Oct 2014 – Feb 2015, c) five-month average May 2015 – Sep 2015, d) five-month average Oct 2015 – Feb 2016

S3. Forecast plumes

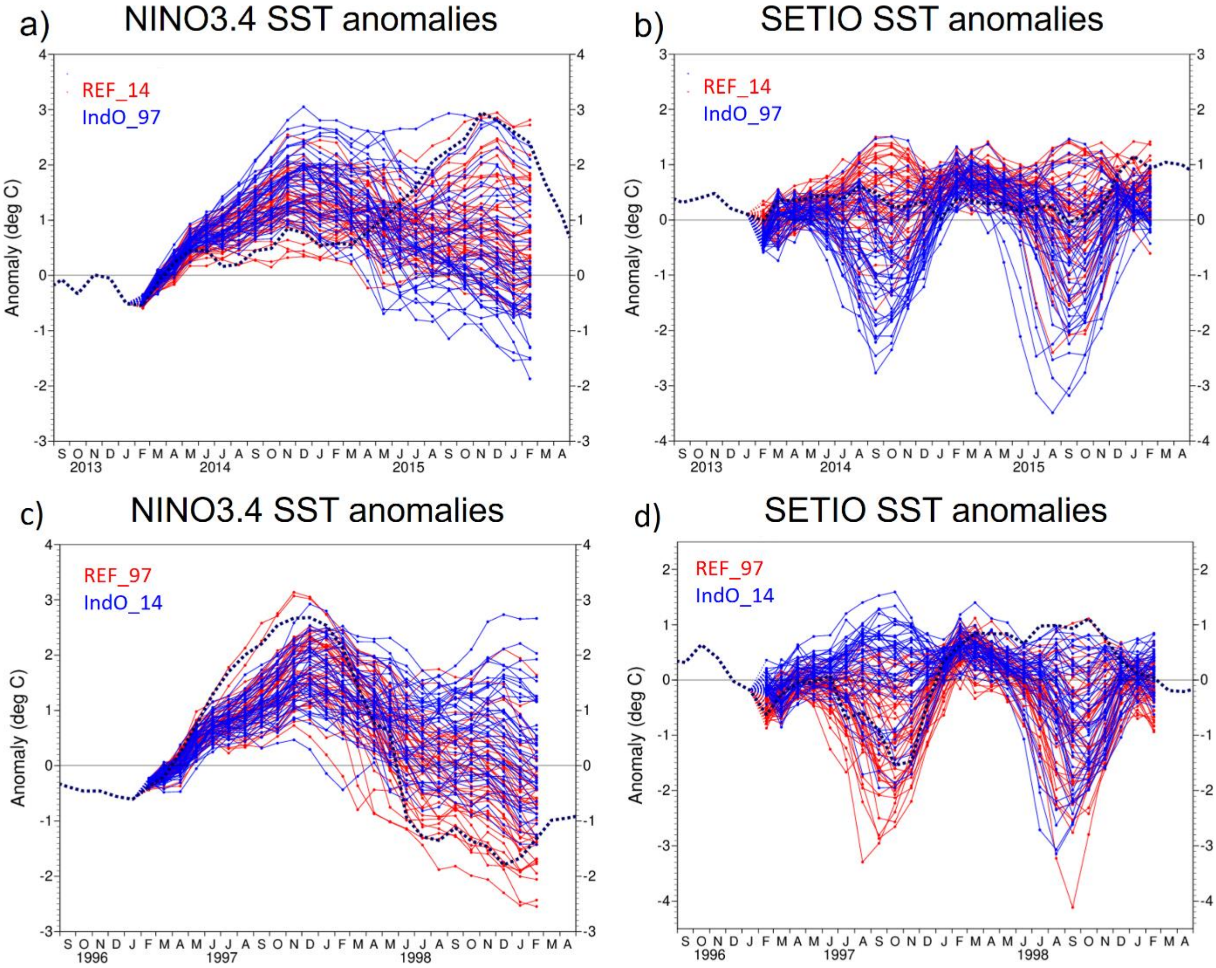

Fig. S3. SST anomalies forecast plumes for Niño 3.4 (left column) and SETIO (right column) from forecast experiments initialized on 1st of February 2014 (top) and 1997 (bottom). The individual ensemble members of REF_14 and REF_97 are shown in red, IndO_97 and IndO_14 in blue, and the observed anomalies (taken from ORAS5) in black. Forecast anomalies are w.r.t model climatology (estimated from AllO_scrambled).

S4. Diagnostics on Nino 3.4 and SETIO SST spread

The Indian Ocean initial conditions also affect the Y1 and Y2 spread of the SST forecast of ENSO and IOD. This is illustrated in Fig. S4, which shows a scatter diagram of the SST forecast spread of experiments with Indian Ocean initial conditions from 1997 on they-axis versus the values from experiments with Indian Ocean from 2014 on the x-axis. The experiments are paired such that they share the same ocean initial conditions everywhere else, yielding four pairings. Results are shown for the spread in the South-Eastern Tropical Indian Ocean (SETIO; averaged over 90-110E, 0-10S) in Aug-Sep-Oct (Y1,Y2) and Niño3.4 in Nov-Dec-Jan (Y1,Y2). It is evident that the forecasts with 2014 Indian Ocean conditions exhibit systematically lower spread in the two regions in both 1997 and 2014. We speculate that reduction of the spread with the 2014 Indian Ocean initial conditions in the SETIO region is associated with the non-occurrence of a positive IOD event (see also Fig. 4 in the main text), which is more predictable than the occurrence of a positive event. Indeed, the correlation between ensemble mean SST anomalies and SST spread across REF_14, IndO_14, AllO_14 REF_97, IndO_97, and AllO_97 is r=-0.97. This relationship is also present in forecasts from SEAS5 initialized in Feb 1993-2016, which exhibit a negative linear relationship between SST forecast spread and anomalies in SETIO (r=-0.73 for Aug-Sep-Oct averages; not shown). The impact of the SETIO spread on Niño 3.4 spread must be via the atmospheric bridge, i.e. through the spread in the Walker Circulation induced by spread in Indian Ocean convection. The changes in Niño 3.4 spread shows that changes in the Indian Ocean can play a role in ENSO predictability, in addition to changes in the Pacific itself.

In summary, results from all experiments using Indian Ocean initial conditions from 1997 show higher SST spread in the Indian Ocean at least from fall 2014 and subsequently also in the Pacific. This suggests that the Indian Ocean conditions in 2014 were rather stable compared to other years and not susceptible to perturbations, which acted to damp instabilities and consequently spread. The results also suggest that the non-occurrence of an IOD event in 2014 was highly predictable, but the occurrence of the event (favoured with 1997 Indian Ocean conditions), is less predictable.

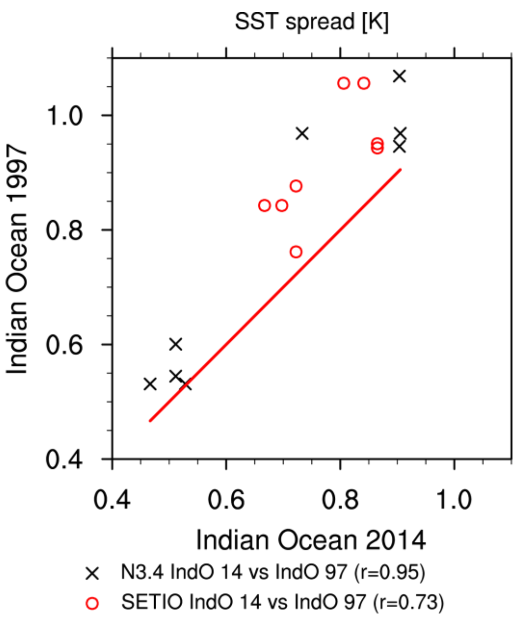

Fig. S4 Spread of forecast of SST in experiments with 1997 Indian Ocean Initial Conditions (not to be confused with experiment IndO_97) versus the spread in experiments with 2014 Indian Ocean Initial

Conditions (not to be confused with experiment IndO_14) The four experiment pairings are (REF_14/ IndO_97; All_14/IndO_97; IndO_14/REF_97; IndO_14/AllO_97). Shown are values for SETIO in Aug-Sep-Oct of Y1 and Y2 (yielding eight circles) and Niño3.4 in Nov-Dec-Jan of Y1 and Y2 (yielding eight crosses)